Pré-Publicações do Departamento de Matemática
Universidade de Coimbra
Preprint Number 15–39

MATHEMATICS OF AGING: ILLNESSES OF THE POSTERIOR SEGMENT OF THE EYE

J.A. FERREIRA, P. DE OLIVEIRA, P.M. DA SILVA AND R. SILVA

Abstract: The changes caused by aging affect all body tissues. The vitreous humor, which fills the space between the lens and the retina, progressively liquefies and shrinks, eventually causing a posterior vitreous detachment. In this work a mathematical model of an aging eye is presented and the influence of retina diseases and aging changes are analyzed. The model is represented by a set of coupled systems of partial differential equations describing the transport of drug in the vitreous chamber. Numerical simulations are compared with experimental results.

1. Introduction

Delivery of drugs to the retina remains a crucial challenge because retinal disorders are major causes of irreversible vision loss leading to blindness.

In diseases of the posterior segment of the eye, intraocular drug delivery systems represent an election treatment because eye drops and systemic administration cannot deliver drug continuously and for long periods of time into the vitreoretinal tissue. Systems clinically successful are based on intraocular injections and non-biodegradable or biodegradable implants, loaded with drug, which are currently used as slow release devices, delivering locally drug for an extended period of time. The influence of age-related changes on the distribution of drugs after intravitreal administration is an area of active research.

In this paper we will present a mathematical model that describes the pharmacokinetics of a drug delivered by an intravitreal biodegradable implant in unhealthy situations.

The vitreous humor is a clear gel that occupies the posterior compartment of the eye, between the lens and the retina. It maintains the shape of the eye,

Received October 12, 2015.

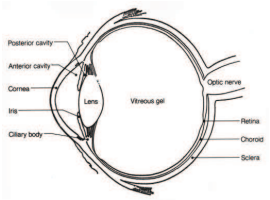

FIGURE 1. Anatomy of the eye ($http://usercontent1.hubimg.com$).

supplies it with nutrition and helps with the focusing of light. The vitreous humor is composed of 99% water by weight, and the other 1% is made up of special substances - collagen and hyaluronic acid-which give the vitreous its gel-like consistency. Drug molecules migrate from the polymeric implant, inserted in the vitreous, to the retina. The distribution of drug depends on multiple factors as the type and severity of retinal disorders, the properties of the release medium, that is the vitreous humor, the physicochemical properties of the drug and the characteristics of the polymer. The purpose of our work is to study, from a mathematical point of view, how such disease conditions, influence the pharmacokinetics of a drug.

Normally, the back surface of the vitreous, called the hyaloid, is in direct contact with the retina (Figure 1). With aging the vitreous gel exhibits a heterogeneous structure characterized by a space dependent permeability. It becomes more fluid, undergoing syneresis and forming liquid pockets called lacunae (Figure 2).

The progressive liquefaction of the vitreous leads to lacunae coalescence which is normally followed by a decreasing in the adhesion of the vitreous with the retina. The separation of the posterior hyaloid face from the retina can then occur: first partially and then totally. This separation is called a Posterior Vitreous Detachment (PVD). In Figure 3 we exhibit a vitreous detachment process. In the top a vitreous completely attached is represented. In the middle a partially detached vitreous is represented and in the bottom a complete PVD is shown.

Instituto Politécnico de Coimbra, ISEC, DFM, Rua Pedro Nunes, 3030-199 Coimbra, Portugal. CMUC.

E-mail address: pascals@isec.pt

R. Silva

Faculty of Medicine, University of Coimbra, Portugal (FMUC); Department of Ophthalmology, Centro Hospitalar e Universitário de Coimbra, Portugal (CHUC); Association for Innovation and Biomedical Research on Light and Image, Coimbra, Portugal (AIBILI)

E-mail address: rufino.silva@oftalmologia.co.pt

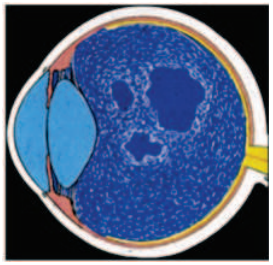

Figure 2. With aging vitreous humor forms liquid pockets called lacunae (*http* : *//retinaspecialists.com.au/wp* − *content/uploads/*2013/04/*new*10.*jpg*).

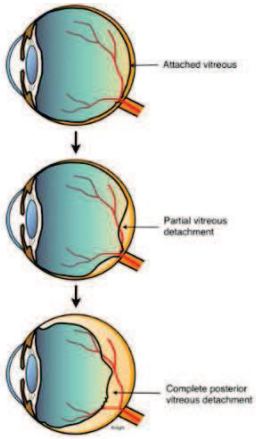

Figure 3. Evolution of posterior vitreous detachment - top - vitreous completely attached, middle - partially detached vitreous, bottom - complete posterior vitreous detachment (*http* : *//images.netdoctor.co.uk/ukcuk*892000000$_{v}$*itreous* − *detachment.jp*).

While in a healthy situation the vitreous chamber is completely filled with a homogeneous vitreous gel, in the case of occurrence of lacunae and/or PVD, the pressure gradients caused by these new patterns can alter the

pharmacokinetics of the drug, raising concern in the medical community about the drug delivery trend.

However at the best of our knowledge no solid conclusions have been established until now regarding the effect of liquefaction on intravitreal pharmacokinetics. Without being exhaustive we mention two papers, where experimental results are presented, leading to a different conclusion. In [9] the authors conclude that the occurrence of a PVD, in vitrectomized and non vitrectomized eyes, does not alter the pharmacokinetics of the drug. On the contrary in [15] the authors, while studying drug diffusion in a liquefied vitreous, conclude that meaningful differences are observed. A better understanding of the impact of aging conditions is necessary to develop more effective therapies so that drug concentration can be maintained within the therapeutic window at the target site. Mathematical models that simulate real physiological conditions are of great help in laboratory experiments and can represent an important contribution for medical doctors while providing guidance for future implant development.

The existence of retinal inflammation, the liquefaction of the vitreous and posterior vitreous detachment are modelled in the present paper and their influence in the redistribution of drug is studied. In previous papers, by some of the authors ([4], [10]), the pharmacokinetics of a drug released from a biodegradable implant was studied in the case of a healthy vitreous, completely attached to the anterior face of the retina. The transport of drug, released by an intravitreal injection, in a homogeneous, completely attached vitreous has been considered in [13].

These last years there has been a certain controversy regarding the differences between the transport of a drug in a healthy vitreous and a liquefying vitreous with or without a detachment. Two main explanations have been considered to justify a larger rate of distribution of drug molecules suggested by some *in vitro* and *in vivo*. The first is a substantial reduction in viscosity of a liquefied vitreous humor, which leads to an increase in effective diffusion of drug ([1]). However other authors consider that this explanation is based

on Computational and Mathematical Methods in Science and Engineering, CMMSE 2015, 2015.

[11] N. Haghjou, M.J. Abdekhodaie, Y.L. Cheng. M. Saadatmand, Computer modeling of drug distribution after intravitreal administration, W.A.S. Engineering and Tecnology 53 (2011) 706–716.

[12] Jing Xu , Jeffrey J. Heys , Victor H. Barocas , Theodore W. Randolph, Permeability and Diffusion in Vitreous Humor: Implications for Drug Delivery, Pharmaceutical Research, Volume 17, Issue 6 , pp 664-669.

[13] J. Kathawate and S. Acharya, Computational modeling of intravitreal drug delivery in the vitreous chamber with different vitreous substitutes, International Journal of Heat and Mass Transfer 51 (2008) 5598–5609.

[14] L.L. Lao, S.S. Venkatraman, N.A. Peppas, Modeling of drug release from biodegradable polymer blends, European Journal of Pharmaceutics and Biopharmaceutics 70 (2008) 796–803.

[15] Lay Ean Tan, Werhner Orilla, Patrick M. Hughes, Susan Tsai, James A. Burke, Clive G. Wilson, Effects of Vitreous Liquefaction on the Intravitreal Distribution of Sodium Fluorescein, Fluorescein Dextran, and Fluorescent Microparticles, Investigative Ophthalmology and Visual Science, Vol.52 (2011) 1111-1118.

[16] M.S. Stay, J. Xu, T.W. Randolph, and V.H. Barocas, Computer simulation of convective and diffusive transport of controlled-release drug in the vitreous humor, Pharmaceutical Research, 20(1) (2003) 96–102.

[17] Stefánsson E, Loftsson T, The Stokes-Einstein equation and the physiological effects of vitreous surgery, Acta Ophthalmol Scand., 84(6), (2006) 718-719.

[18] S. Rothstein, W.Federspiel, S. Little, A unified mathematical model for the prediction of controlled release from surface and bulk eroding polymer matrices, Biomaterials 30 (2009) 1657–1664.

[19] T. Yasukawa, Y. Ogura, H. Kimura, E. Sakurai, Y. Tabata, Drug delivery from ocular implants, Expert Opin Drug Deliv. 3 (2006) 261–273.

J.A. Ferreira
CMUC-Department of Mathematics, University of Coimbra, Apartado 3008, 3001-454 Coimbra, Portugal

E-mail address: ferreira@mat.uc.pt
URL: http://www.mat.uc.pt/~ferreira

P. de Oliveira
CMUC-Department of Mathematics, University of Coimbra, Apartado 3008, 3001-454 Coimbra, Portugal

E-mail address: poliveir@mat.uc.pt

P.M. da Silva

role becomes important in complementing *in vivo* experiments and helping them to become more relevant to actual clinical situations.

Acknowledgements

This work was partially supported by the Center for Mathematics of the University of Coimbra - UID/MAT/00324/2013, funded by Portuguese Government through FCT/MEC and co-funded by through the Partnership Agreement PT 2020.

References

[1] Andrew R.H. Simpson, Robert Petrarca, Timothy L. Jackson, Vitreomacular Adhesion and Neovascular Age-Related Macular Degeneration, Survery of Ophthalmology, vol. 57(6) (2012) 498-509.

[2] Annie Chan, Loh-Shan Leung, and Mark S Blumenkranz, Critical appraisal of the clinical utility of the dexamethasone intravitreal implant (Ozurdex) for the treatment of macular edema related to branch retinal vein occlusion or central retinal vein occlusion, Clin Ophthalmol, vol. 5 (2011) 1043-1049.

[3] M. A. Akhmanovaa, S. P. Domogatskyb, and V. Yu. Evgrafovc, Computer Simulation of Hydraulic Flows in the Human Eye, Biophysics, Vol. 56 (2011) No. 1, pp. 108-113

[4] E. Azhdari, J.A. Ferreira, P. de Oliveira, P.M. da Silva, Diffusion, viscoelasticity and erosion: analytical study and medical applications, Journal of Computational and Applied Mathematics, 275, (2015) 489-501.

[5] E. Azhdari, J.A. Ferreira, P. de Oliveira, P.M. da Silva, Numerical and analytical study of drug release from a biodegradable viscoelastic platform, Mathematical Methods in Applied Sciences, (2015), DOI: 10.1002/mma.3375.

[6] R.K. Balachandran, V.H. Barocas, Computer modeling of drug delivery to the posterior eye: effect of active transport and loss to choroidal blood flow, Pharmaceutical Research 25 (2008) 2685–2696.

[7] R.K. Balachandran and V.H. Barocas, Finite element modeling of drug distribution in the vitreous humor of the rabbit eye, Annals of Biomedical Engineering 25 (1997) 303–314.

[8] Barton, K. A., Shui, Y.B., Petrash, J. M., Beebe, D. C., Comment on: the Stokes-Einstein equation and the physiological effects of vitreous surgery. Acta Ophthalmologica Scandinavica, 85(3), (2007) 339-340.

[9] Chang-Lin JE, Burke JA, Peng Q, et al., Pharmacokinetics of a sustained-release dexamethasone intravitreal implant in vitrectomized and nonvitrectomized eyes. Invest Ophthalmol Vis Sci. 53 (2011) 4605–4609.

[10] J.A. Ferreira, P. de Oliveira, P.M. da Silva, R. Silva, A mathematical model of controlled drug release in a completely detached vitreous , Proceedings of the 15th International Conference

on the Stokes-Einstein equation that describes the effect of the viscosity on the rate of diffusion of small molecules in a liquid and not in a gel ([17]). They claim that the diffusion coefficients of different molecules (small and large molecular weight) measured in saline solutions or vitreous gel are similar. Their alternative explanation for the increased rate at which molecules are redistributed in a liquefied vitreous is more likely to be a consequence of an increase in fluid circulation than a difference in the rate of diffusion ([8]).

Following this last approach we consider that the driving phenomena involved in controlled drug delivery from a bioerodible implant, through the vitreous chamber are diffusion, convection and polymeric degradation. Convection arises due to a flow driven by a pressure gradient between the hyaloid membrane and the posterior retina surface. Experimental results state that convection contributes with around 30% of the total intravitreal transport ([12]). For large molecular weights the contribution should increase, because diffusion coefficients are smaller; the same is true for glaucomatous eyes, where higher intraocular pressure occurs raising a larger convection rate. On the contrary, for hypertensive patients, such contribution should be less significant because the blood pressure approaches the intraocular pressure and consequently the pressure gradient is smaller.

The mathematical model presented in this paper is represented by four coupled systems of partial differential equations describing the transport of drug in the implant, the vitreous humor, the space filled with aqueous humor, which has been created by the detachment, and the retina (Figure 3). We analyze the influence of the physiological conditions that characterize a liquefying, detached vitreous and an inflamed retina and compare the pharmacokinetics of a drug in this situation with the pharmacokinetics of a healthy vitreous.

In Section 2 we present the geometry and the coupled model that describes the evolution of drug concentration in the implant, the vitreous, the detachment region and the retina. A mass balance of drug is also established. In Section 3 we study the dependence of the pharmacokinetics on the degree

of inflammation of the retina and the degree of vitreous permeability. The transport of drug in case of Posterior Vitreous Detachment is also addressed. Finally in Section 4 we discuss the results and present some conclusions.

2. Mathematical model

2.1. Geometry of the model. The vitreous chamber is represented in Figure 4 by $\Omega_2 \cup \Omega_3$. In normal conditions it is filled by vitreous humor and it occupies about two-thirds of the eye. The lens, also called crystalline lens, acts to focus images in the retina. It is modeled in Figure 4 as an ellipsoid. The hyaloid membrane and the lens separate the anterior chamber and the posterior chamber of the eye from the vitreous chamber. The retina, Ω_4, forms the boundary of the vitreous chamber on the posterior surface and is modeled as the volume between two spherical surfaces with radius differing of 11 mm. We assume that the retina is a porous tissue with external boundary represented by $\partial\Omega_{out}$. In this boundary we assume the pressure is 1200Pa; in the interface that represents the hyaloid membrane, $\partial\Omega_{in}$, we consider a pressure of 2000 Pa. The pressure in $\partial\Omega_{in}$ corresponds to a normal intraocular pressure in the anterior chamber of the eye; the pressure in $\partial\Omega_{out}$ corresponds to a normal mean blood pressure. This pressure gradient is responsible for the convection flow between the anterior part of the vitreous chamber and its posterior part.

In Figure 4 we represent a Posterior Vitreous Detachment (PVD). The detachment zone created by the PVD is naturally filled with liquefied vitreous humor. In Figure 4 that zone is represented by Ω_3. The vitreous humor gel shrinks, separates from the retina and occupies Ω_2. To treat diseases of the posterior chamber of the eye one of the gold standard treatments is controlled release from an intravitreal implant, Ω_1, that can be bioerodible or non bioerodible*. In the model presented in this paper the implant is considered bioerodible. This intravitreal implant containing dispersed drug

*At present both types of intravitreal implants - biodegradable and no biodegradable - are commercialized by pharmaceutical companies.

time is shorter and the peak of concentration is smaller. We observe that after fours months of release the concentration in the case of a normal vitreous is approximately the double of PVD - IC. This difference is more meaningful than the observed in Figure 11, where the beginning of a liquefying process is depicted.

4. Conclusion

The aim of this paper is to answer the following question: what are the main differences in the pharmacokinetics of a drug in the case of anomalies of the vitreous humor due to aging and retina diseases? Three cases are analysed: inflammation of the retina, liquefaction of the vitreous humor and posterior vitreous detachment.

Concerning the inflammation of the retina it is shown in subsection 3.1 that as it progresses the concentration peak and the residence time decrease.

No significant differences occur in the concentration in the early states of liquefaction (subsection 3.2), when we assume that clearance is not affected by the process. However if liquefaction is accompanied by an increase of the clearance as stated in clinical work [15] the concentration peak is achieved earlier and the residence time is shorter.

In the case of PVD, analogous results are obtained. The combined effect of a larger convective flow (Figure 12) and an increase in the clearance of the retina explain that short residence times are observed (Figure 14).

A final conclusion that arises from Figure 11 and Figure 14 is that as aging progresses the peak and the residence time are shorter. This is an interesting outcome for manufacturers and medical doctors that can help to pave the way for a personalized medicine.

In vivo experiments often use juvenile animal models with no alterations in the vitreous structure. As pointed in [15] the data obtained from these experiments can overestimate drug efficacy. As mathematical model can tune with a certain accuracy the parameters that govern the effects of aging their

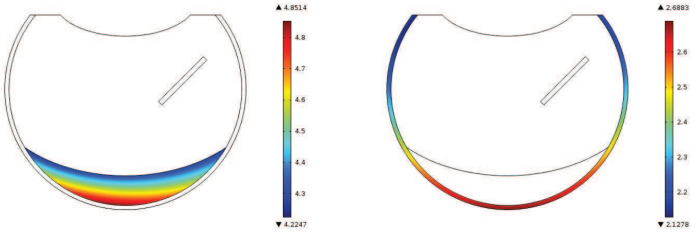

FIGURE 13. Distribution of drug concentration after 4 months of released in the detached zone (left) an retina (right).

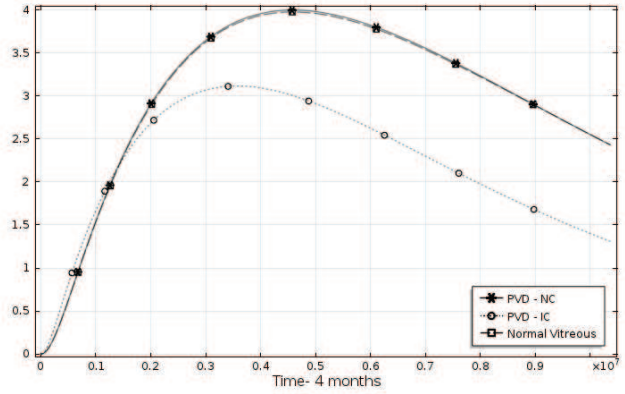

FIGURE 14. Drug concentration in the retina during 4 months: in the case of a normal vitreous, a Posterior Vitreous Detachment with Normal Clearance(PVD-NC) and Increased Clearance (PVD-IC).

We now compare, in Figure 14, the pharmacokinetics of a drug in a completely attached vitreous (Normal Vitreous) and a vitreous with a posterior detachment (PVD - NC). Unexpectedly the two plots are practically indistinguishable. This numerical result is in agreement with the experimental results in [9]. If an increased clearance is considered (PVD - IC) the residence

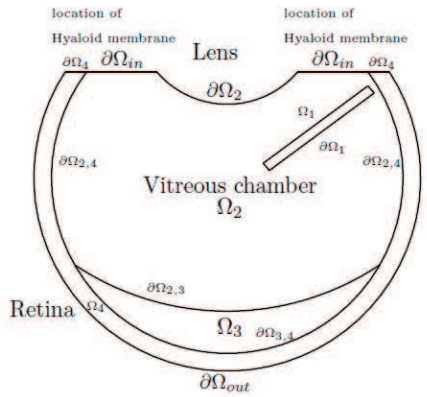

FIGURE 4. Geometry of the posterior segment of the eye: the implant, Ω_1, inside the vitreous chamber; the vitreous humor, Ω_2, occupying part of the vitreous chamber; the region Ω_3 caused by the detachment of the vitreous humor; the retina, Ω_4.

is placed in the vitreous, near the retina (Figure 4). It is geometrically represented by a cylinder with radius 0.023 mm and height 0.6 mm. The drug is released in a controlled manner into the vitreous which is a porous media, and its target is the retina affected by an inflammatory process.

The geometrical model described in this Section has been partially presented by the authors in [10]. However the problems studied in the present paper - inflammation of the retina, liquefaction of the vitreous - have not been addressed in the previous work. The influence of a PVD is analyzed in [10], nevertheless only a diffusive transport is assumed in the retina. In this paper the transport in the retina is described by a convection-diffusion equation where the convection rate is defined by Darcy's Law. A boundary condition in the pressure (normal blood pressure 1200 Pa) is considered in $\partial\Omega_{out}$. This modeling difference - a pure diffusive transport of drug in [10]

and a convection-diffusion transport in the present paper - leads to a more realistic description of the behavior of drug concentration in the retina.

2.2. Equations of the model. An initial amount of drug is dispersed in the polymeric implant Ω_1. We suppose that when in contact with the vitreous humor an instantaneous swelling occurs. The drug then dissolves and is transported through the implant, the vitreous chamber and the retina.

The model presented in this paper results from the coupling of four systems of partial differential equations, each one representing the transport of drug in those isotropic regions.

- Transport in the implant Ω_1

Assuming that only passive transport takes place in the biodegradable polymeric implant, the concentration of drug, C_1, and the molecular weight, M, of the biodegradable polymer are described by

$$\begin{cases} \dfrac{\partial C_1}{\partial t} = \nabla \cdot (D_1(M)\nabla C_1) \text{ in } \Omega_1 \times (0,T], \\ \dfrac{\partial M}{\partial t} + \beta_1 M = \beta_2 C_1 \text{ in } \Omega_1 \times (0,T], \end{cases} \tag{1}$$

where $D1$ stands for the diffusion coefficient of the drug in the polymeric implant, depending on M, and β_1, β_2 are physical constants that characterize the degradation properties of the material. It is expected that as the polymer erodes, the molecular weight M decreases and the diffusion coefficient of the drug increases. To describe this behavior we define

$$D_1(M) = D_0 e^{\overline{k}\frac{M_0 - M}{M_0}}, \tag{2}$$

where D_0 is the diffusion coefficient of the drug in the non hydrolyzed polymer, $\overline{k}$ is a positive constant and M_0 is the initial molecular weight of the polymeric matrix ([18], [4], [10]). As $M_0 > M$ we have $D_1(M) > D_0$.

In the case of a PVD, analysed in subsection 3.3, the transport in the vitreous chamber is governed by different equations in Ω_2 and Ω_3. This is

lost and the drug flow must permeate a space filled with aqueous humor (PVD) before reaching the retina (Figure 4).

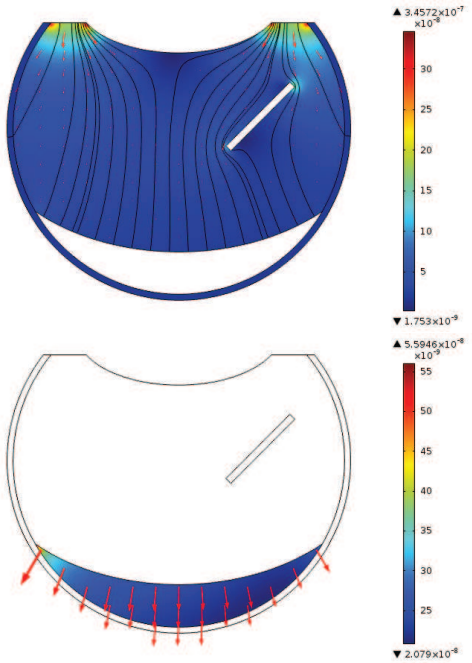

FIGURE 12. Velocity fields in the vitreous (up) and the detached zone (down).

In Figure 12 we exhibit the velocity fields of the fluid in the vitreous chamber: the velocity is higher in the detached zone (Figure 12 bottom) than in the vitreous humor (Figure 12 top).

The concentration of drug after 4 months of release is shown in Figure 13. In Figure 13 (left) the non-diffusive character of the pattern exhibits evidence of a transport dominated by convection. We observe that the scales in both plots are different and that a discontinuity in the concentration - between the detached zone and the retina - is visible.

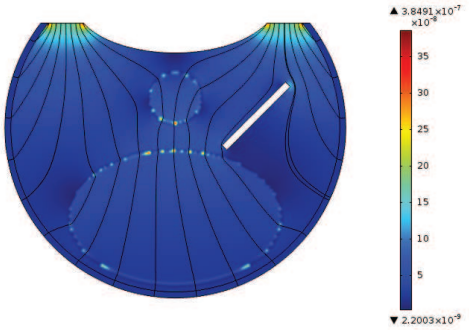

FIGURE 10. Velocity in the vitreous when a liquefaction of the vitreous occurs.

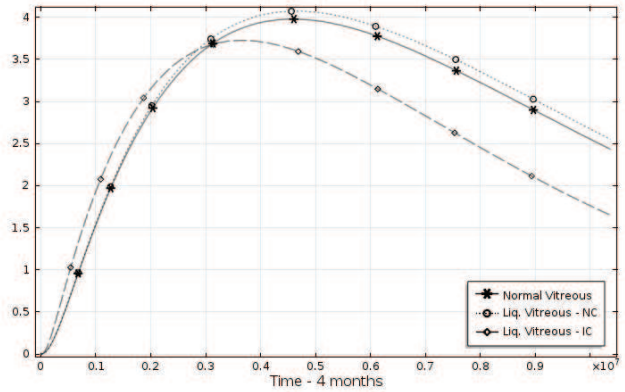

FIGURE 11. Drug concentration in the retina during 4 months, in a normal vitreous, a liquefying vitreous with normal clearance (LV-NC) and a liquefying vitreous with an increased clearance (LV-IC).

3.3. Posterior Vitreous Detachment. Age-related weakening of adhesions between vitreous and retina often leads to posterior vitreous detachment. The direct contact between the vitreous humor and the retina is then

due to the fact that Ω_2 is occupied by vitreous humor gel and Ω_3 is filled with liquefied vitreous humor.

- Transport in the vitreous humor Ω_2

The aqueous humor flow through the vitreous chamber has been a controversial topic for many years. Nowadays it is commonly accepted that there is a movement of aqueous humor in the vitreous chamber. The vitreous humor has a porous structure and the drug is transported by diffusion, with a coefficient D_2, and by convection with a velocity $\mathbf{v}_2$ induced by the difference of pressure p_2 between the hyaloid membrane ($\partial\Omega_{in}$) and the interface with the detachment zone ($\partial\Omega_{2,3}$). The behavior of the concentration is described by the equations

$$\frac{\partial C_2}{\partial t} + \nabla \cdot (C_2 \mathbf{v}_2) - \nabla \cdot (D_2 \nabla C_2) = 0 \,\texttt{in}\, \Omega_2 \times (0, T], \tag{3}$$

and

$$\begin{cases} \mathbf{v}_2 = -\dfrac{K}{\mu_1} \nabla p_2 \,\texttt{in}\, \Omega_2 \times (0, T] \\ \nabla \cdot \mathbf{v}_2 = 0 \,\texttt{in}\, \Omega_2 \times (0, T] \end{cases}. \tag{4}$$

In equation (3) C_2 represents the concentration of the drug in the vitreous humor, D_2 is the diffusion coefficient of the drug in the vitreous and $\mathbf{v}_2$ is the permeation velocity of aqueous humor given by Darcy's equation (4). In this last system K is the permeability of the vitreous and μ_1 is the viscosity of the permeating aqueous humour ([13]).

- Transport in the detachment zone Ω_3

When a PVD occurs a detachment zone, Ω_3, forms in the vitreous chamber $\Omega_2 \cup \Omega_3$.

The concentration of drug in Ω_3 is described by a convection-diffusion equation. As this zone is filled with liquefied vitreous humor, which composition is 99% of water, Navier-Stokes equation is used to model the velocity. The evolution of drug concentration is then described by

$$\frac{\partial C_3}{\partial t} + \nabla \cdot (C_3 \mathbf{v}_3) - \nabla \cdot (D_2 \nabla C_3) = 0 \texttt{ in } \Omega_3 \times (0,T], \tag{5}$$

where the velocity $\mathbf{v}_3$ is given by the Navier-Stokes equations

$$\begin{cases} \rho \dfrac{\partial \mathbf{v}_3}{\partial t} - \nabla . \mu_1 (\nabla \mathbf{v}_3 + (\nabla \mathbf{v}_3)^T) + \rho (\mathbf{v}_3 . \nabla) \mathbf{v}_3 + \nabla p_3 = 0 \texttt{ in } \Omega_3 \times (0,T], \\ \nabla . \mathbf{v}_3 = 0 \texttt{ in } \Omega_3 \times (0,T]. \end{cases} \tag{6}$$

In equation (5), C_3 represents the drug concentration in Ω_3 and D_2 represents the drug diffusion coefficient in the vitreous humor. The variables p_3 and $\mathbf{v}_3$ in (6) stand for the pressure and the velocity of the fluid in Ω_3, respectively and ρ stands for the density of the fluid.

If no PVD occurs, as the situations addressed in subsections 3.1 and 3.2, then the vitreous humor occupies the vitreous chamber, $\Omega_2 \cup \Omega_3$, and $\partial\Omega_{2,3}$ is a virtual line that doesn't act as an interface. The flow in the vitreous chamber is then described by equations (3) and (4).

- Transport in the retina Ω_4

The target organ for the drug released from the intravitreal implant is the retina. The behavior of the drug concentration in the retina is simulated considering the following equations

$$\frac{\partial C_4}{\partial t} + \nabla \cdot (C_4 \mathbf{v}_4) - \nabla \cdot (D_2 \nabla C_4) = 0 \texttt{ in } \Omega_4 \times (0,T], \tag{7}$$

and

$$\begin{cases} \mathbf{v}_4 = -\dfrac{K_r}{\mu_r} \nabla p_4 \texttt{ in } \Omega_4 \times (0,T] \\ \nabla \cdot \mathbf{v}_4 = 0 \texttt{ in } \Omega_4 \times (0,T] \end{cases} . \tag{8}$$

In equation (7) C_4 represents the concentration of drug in the retina Ω_4 and $\mathbf{v}_4$ is the velocity of fluid permeation given by Darcy's equation (8). In this last system K_r represents the permeability of the retina, μ_r the viscosity of the fluid and $\frac{K_r}{\mu_r}$ is the hydraulic conductivity of the retina ([13]).

3.2. Liquefaction of the vitreous humor. In this subsection a completely attached vitreous with a space dependent permeability is studied. The heterogeneity of the vitreous is represented geometrically by two regions with a larger permeability that will affect the convection rate (Figure 10). This scenario corresponds to an early state of vitreous liquefaction where lacunae haven't yet occurred. Regions of higher permeability will give rise to such fluid pools.

In Figure 10 we plot the velocity of the fluid in the vitreous. Comparing the scales of the velocity fields in Figure 6 and Figure 10 we observe that lower velocities occur in Figure 6. We recall that in this case the vitreous humor is homogeneous and has a smaller permeability than the heterogeneous vitreous represented in Figure 10. This fact suggests a higher mean concentration of drug in the retina, when a normal clearance is considered, as shown in Figure 11 (Normal vitreous *vs* liquefying vitreous - NC). However the difference is very slight. The result agrees with the conclusion of the experimental work presented in [9]. It is known that as the liquefaction of the vitreous gel takes place, the clearance of the retina increases ([15]). The liquefaction is accompanied by the hydrolysis of the hyaluronic acid that cause inflammation in the retina, increasing the rate of clearance. Considering an increased clearance, the concentration plot (liquefying vitreous - IC) is exhibited in Figure 11. The concentration peak is achieved approximately after one month of the implant insertion. The residence time is shorter. The concentrations levels are smaller. This result agrees with the conclusions in [15] where the authors claim that in elderly population higher drug dosages are needed, when comparing with younger individuals.

A possible explanation of these different experimental results ([9] and [15]) can be related to the use of juvenile animal models that underestimate the influence of vitreous liquefaction. The role of mathematical models, providing numerical simulations for a set of parameters that mimic different vitreous ages, can be of great help in guiding *in vivo* experiments.

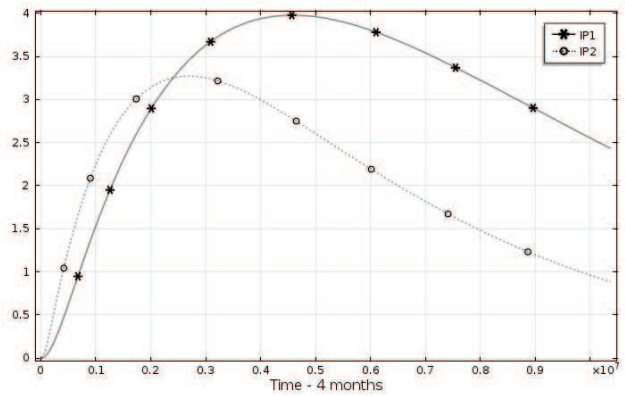

FIGURE 8. Influence of retina inflammation in the drug concentration in the retina during 4 months.

(cm^2/h) ([1]). In Figure 9 we exhibit the concentration plots when IP1 occurs, for drugs with different molecular weights and consequently different diffusion coefficients. We note that as the diffusion coefficient increases the concentration peak decreases.

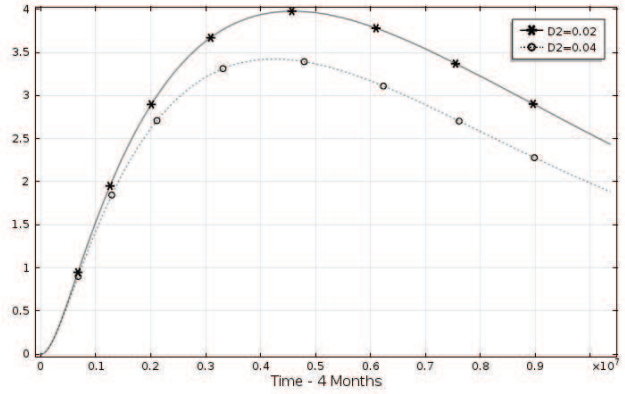

FIGURE 9. Influence of the diffusion coefficient in the drug concentration in the retina during 4 months .

We note that the diffusion coefficient of the drug is represented by D_2 in Ω_i, $i = 2, 3, 4$, because it is assumed that the drug diffuses in the fluid that circulates in these regions. We recall that this fluid is composed by aqueous humor and liquefied vitreous gel. This modelling choice is based on [8]. However the properties of the transport are different in these domains because the convection rate is governed by different laws: Darcy's law in Ω_2 and Ω_4; Navier-Stokes equations in Ω_3.

To complete the model initial, boundary and interface conditions are added.

- Initial conditions

Initial conditions for the concentrations account for the fact that at $t = 0$ the concentration of drug is zero everywhere except in the implant, that is

$$\begin{cases} C_1(0) = C_0 \,\texttt{in}\, \Omega_1, \\ C_2(0) = 0 \,\texttt{in}\, \Omega_2, \\ C_3(0) = 0 \,\texttt{in}\, \Omega_3, \\ C_4(0) = 0 \,\texttt{in}\, \Omega_4. \end{cases} \tag{9}$$

In the case of a PVD, Navier-Stokes equation is coupled with an initial velocity. The initial condition for velocity in the detached zone is

$$v_3(0) = 0 \,\texttt{in}\, \Omega_3. \tag{10}$$

- Boundary conditions and interface conditions

- For the pressure: $p = 2000 \,\texttt{on}\, \partial\Omega_{in}$ and $p = 1200 \,\texttt{on}\, \partial\Omega_{out}$. We note that $\partial\Omega_{in}$ represents the hyaloid membrane and $\partial\Omega_{out}$ represents the interface of the retina with the choroid. These two values of the pressure correspond to a normal intraocular pressure in the anterior chamber near the lens and a normal blood pressure, respectively.
- For the velocity: $\mathbf{v} \cdot \eta = 0$ on the boundaries $\partial\Omega_1$, $\partial\Omega_2$, $\partial\Omega_4$ (Figure 4). In this last equation $\mathbf{v}$ and η represent the velocity and the unit exterior normal to each one of those boundaries, respectively.
- Continuity of the velocity and the pressure in the interface $\partial\Omega_{2,3}$.

- Interface conditions for the fluxes of drug defined by $J_1 = -D_1(M)\nabla C_1$, $J_2 = -D_2\nabla C_2 + \mathbf{v}_2 C_2$, $J_3 = -D_2\nabla C_3 + \mathbf{v}_3 C_3$ and $J_4 = -D_2\nabla C_4 + \mathbf{v}_4 C_4$.

  Implant - Vitreous: $J_1 \cdot \eta = J_2 \cdot \eta, \quad J_1 \cdot \eta = A_1(C_1 - C_2)$ on $\partial\Omega_1 \times (0,T]$, where A_1 is the permeability constant of the polymer and η is the unit exterior normal to Ω_1 on $\partial\Omega_1$;

  In the case no PVD exists, the vitreous humor occupies the vitreous chamber $\Omega_2 \cup \Omega_3$ and the interface line $\partial\Omega_{2,3}$ doesn't exist. An interface condition between the vitreous and the retina is considered:

  Vitreous - Retina: $J_2 \cdot \eta = J_4 \cdot \eta, \quad J_2 \cdot \eta = A_2(C_2 - C_4)$ on $\partial\Omega_{2,4} \times (0,T]$, where A_2 is a permeability constant and η is the unit exterior normal to Ω_2 on $\partial\Omega_{2,4}$.

  When a PVD occurs, two interface conditions replace the vitreous-retina condition previously defined:

  Vitreous - Detachment zone: $J_2 \cdot \eta = J_3 \cdot \eta, \quad C_2 = C_3$ on $\partial\Omega_{2,3} \times (0,T]$, where η is the unit exterior normal to Ω_2 on $\partial\Omega_{2,3}$

  Detachment zone - Retina: $J_3 \cdot \eta = J_4 \cdot \eta, \quad J_3 \cdot \eta = A_3(C_3 - C_4)$ on $\partial\Omega_{3,4} \times (0,T]$, where A_3 is the permeability constant and η is the unit exterior normal to Ω_3 on $\partial\Omega_{3,4}$.

The boundary conditions that follow complete the model.

As the retina is a permeable membrane, it is assumed that $J_4 \cdot \eta = A_4 C_4$, where η is the unit outward normal to Ω_4 on $\partial\Omega_{out}$ and A_4 is a positive constant.

On the contrary, as the lens and the hyaloid membrane are not permeable to the drug, it is assumed that $J_2 \cdot \eta = 0$ on $\partial\Omega_2 \times (0,T]$, and $J_4 \cdot \eta = 0$ on $\partial\Omega_4 \times (0,T]$, where η is the unit outward normal to Ω_2 on $\partial\Omega_2 \cup \partial\Omega_4$.

2.3. Mass conservation. The total mass of drug in the system is represented by

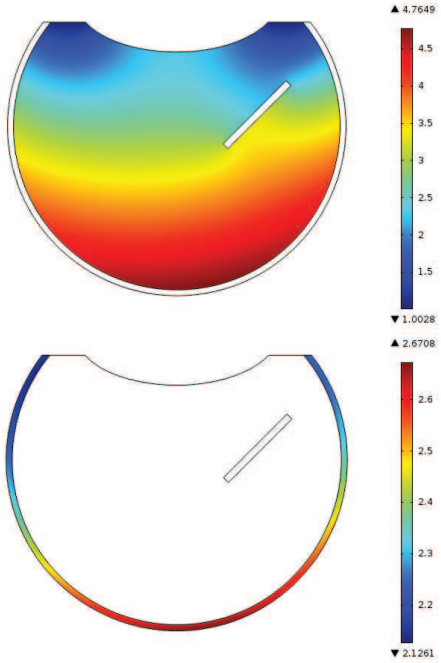

FIGURE 7. Distribution of drug concentration after 4 months of release in the vitreous (up) and retina (down).

in IP2 and the residence time are smaller. The peak in IP1 occurs after 2 months of release. This result is in agreement with [2]. However in a more severe inflammation process as IP2 the peak occurs after one month of release. These results suggest that as inflammation in retina progresses, the concentration peak and the residence time decrease.

We conclude this subsection by observing the influence of the diffusion coefficient. Drugs with small molecular weight have a large diffusion coefficient and convection plays a small role; for drugs with large molecular weight, slower diffusing, convection becomes more important ([16]). The diffusion coefficient of drugs used in retina diseases varies in the interval [0.02, 0.06]

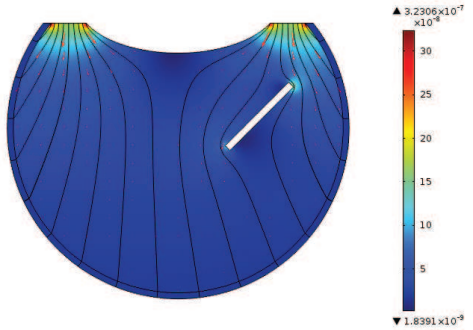

FIGURE 6. Steady state velocity in the vitreous and in the retina.

In Figure 7 we plot the drug concentration in the vitreous chamber and in the retina after 4 months of drug release. On the top we observe that the drug accumulates near $\partial\Omega_{2,4}$, adjacently to the retina. This pattern suggest a convection dominated transport. Even if the continuity of concentration is not used in the boundary interface $\partial\Omega_{2,4}$, a similar pattern of drug distribution is observed in the retina. In the bottom plot we can observe that the drug concentration is higher near the optical nerve (Figure 1).

The evolution of drug concentration in the retina for different degrees of inflammation is illustrated in Figure 8. In an inflammatory process there is an increase of blood flow and of capillary permeability. Consequently we characterize here an inflammatory process using the permeability related parameters. The parameters that control the permeability of the retina are the constant A_2 governing the flux through $\partial\Omega_{2,4}$, the constant A_4 governing the flux on $\partial\Omega_{out}$ and the permeability constant K_r (8). We define two inflammatory process: IP1 ($A_2 = A_4 = 1\times10^{-9}\,(m/s)$, $\frac{K_r}{\mu_r} = 1\times10^{-8}\,(cm/s)$) and IP2 ($A_2 = A_4 = 4\times10^{-9}\,(m/s)$, $\frac{K_r}{\mu_r} = 4\times10^{-8}\,(cm/s)$). Process IP2 represents an advanced state of inflammation when compared with process IP1. We observe that, during the initial uptake, a higher concentration is observed in the retina in IP2. Due to the higher permeability of the retina the outflow is larger than in IP1 and consequently the peak of concentration

$$M(t) = \sum_{i=1}^{4} \int\int_{\Omega_i} C_i(x,y,t)dxdy.$$

Taking the time derivative in the last equation we have from equations (1)-(8)

$$\frac{dM}{dt}(t) = -\sum_{i=1}^{4} \int\int_{\Omega_i} \nabla \cdot J_i dxdy,$$

where the mass fluxes J_i are defined in the previous subsection.

Considering the interfaces and the boundary conditions, we conclude from this last equation that

$$\frac{dM}{dt}(t) = -\int_{\partial\Omega_{out}} A_4 C_4(x,y,t)dS,$$

which means that the decreasing of the total mass of drug in the system is proportional to the permeability of the retina, represented by A_4.

3. Numerical Simulations

In this section we analyze the behavior of drug concentration in the vitreous humor and in the retina and its dependence on different physiological factors as the severity of retina inflammation, the liquefaction of the vitreous and the occurrence of posterior vitreous detachment. Particular attention is devoted to the residence time and the concentration peak.

In the subsections 3.1 and 3.2 we assume that no PVD is present. In this case the transport is driven by passive diffusion in the implant Ω_1 and by convection-diffusion in the vitreous chamber $\Omega_2 \cup \Omega_3$ - that is completely filled with vitreous humor - and in the retina Ω_4. The convection rates are defined by Darcy's law. In subsection 3.1 the influence of retina inflammation is studied. In subsection 3.2 an initial stage of vitreous liquefaction, represented by the existence of higher porosity zones, is addressed.

When a PVD occurs the vitreous chamber is filled with vitreous humor gel in Ω_2 and liquefied vitreous humor in the detached zone Ω_3. This case is considered in subsection 3.3.

The numerical results were obtained with *COMSOL Multiphysics* version 4.2, using a piecewise finite element method, linear for the velocity and the pressure and quadratic for the concentrations. A triangulation automatically generated is used with 19862 elements. To integrate in time, adaptive Backward Differentiation Formulae, with orders between 1 and 2 and adaptive time step is used.

The numerical simulations are obtained with $C_0 = 1.7887\times10^{-6}\ (mol/mm^3)$ and $M_0 = 1\times10^{-6}\ (Da)$, which represent the initial drug concentration and the initial molecular weight in the implant, respectively. All the media are considered isotropic. The diffusion of the drug in the implant is defined considering $D_0 = 1\times10^{-13}$; its diffusion coefficient in the vitreous humor is defined by $D_2 = 5.556\times10^{-10}\ (m^2/s)$. We recall that the diffusion coefficient in the polymer will increase as the molecular weight decreases, that is as degradation occurs.

The following values of the parameters have been considered in the simulations: $K = 8.4\times10^{-10}\ (cm^2)$, $\mu_1 = 0.001\ (Pa.s)$, $\beta_1 = 1\times10^{-7}\ (1/s)$, $\beta_2 = 1\times10^{-10}\ (Dam^3/(mol.s))$, $\overline{k} = 1$, $A_1 = 5\times10^{-11}$, $A_2 = A_3 = A_4 = 1\times10^{-9}\,(m/s)$, $\rho = 1000\ (kg/m^3)$ and $\frac{K_r}{\mu_r} = 1\times10^{-8}\ (cm/s)$. These values have been gathered from the literature ([13]).

3.1. Severity of retina inflammation: convection-diffusion transport. In this subsection we assume that no liquefaction is occurring. The model is then defined by equations (1)-(4), (7) and (8) and completed with initial, interface and boundary conditions.

We begin by computing the steady pressure and velocities in the vitreous humor and in the retina in healthy conditions of the vitreous. In Figure 5 a plot of the pressure distribution is exhibited. We observe that in the vitreous chamber the pressure is almost constant, varying in the interval [1990, 2000],

where the pressure units are in Pascal (Pa). We recall that 2000 Pa is the pressure on $\partial\Omega_{in}$, corresponding to a normal intraocular pressure. On the contrary there is a significant variation in the retina, [1200, 1990]. The value 1200 Pa is the pressure assigned to the outlet boundary of the retina, $\partial\Omega_{out}$, and it corresponds to a normal blood pressure.

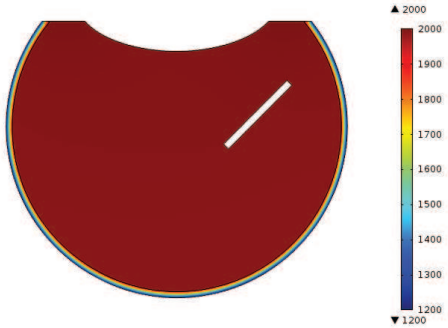

FIGURE 5. Steady state pressure in the vitreous and in the retina.

In a previous paper of the authors [10] a different pattern of the pressure was presented. This is due to the fact that different modelling assumptions were considered. Namely a normal blood boundary pressure of 1200 Pa was defined on $\partial\Omega_{3,4}$, and not in $\partial\Omega_{out}$, because only passive diffusion was taken into account in the retina. As a consequence in [10] the interval of variation of the pressure in the vitreous chamber was [1200, 2000] Pa. The modelling assumptions of the present paper are more realistic, because both diffusion and convection phenomena are considered ([3]).

The velocity field computed using Darcy's law in the vitreous chamber and in the retina is presented in Figure 6. The highest values are observed in the inlet boundary, $\partial\Omega_{in}$, where the aqueous humor enters the vitreous chamber. The mean velocity is of order 10^{-8}. This value is in agreement with values found in the literature ([13], [3]).